NPS-MA-93-010

NAVAL POSTGRADUATE SCHOOL

Monterey, California

ELASTIC CURVES ON THE SPHERE

by

Guido Brunnett
Peter E. Crouch

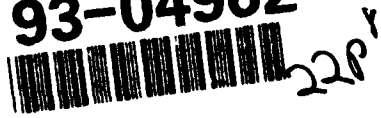

Technical Report For Period
September 1992 - November 1992

Prepared for: Naval Postgraduate School
Monterey, CA 93943

NAVAL POSTGRADUATE SCHOOL
MONTEREY, CA 93943

Rear Admiral T.A. Mercer
Superintendent

Harrison Shull
Provost

This report was prepared in conjunction with research conducted for the Naval Postgraduate School and funded by the Naval Postgraduate School.

This report was prepared by:

G. Brunett

GUIDO BRUNNETT
Post Dr. Associate

Brunett for

PETER E. CROUCH
Professor

Reviewed by:

Richard Franke

RICHARD FRANKE
Chairman

Released by:

P. J. Howard Jr

PAUL J. MARTO
Dean of Research

REPORT DOCUMENTATION PAGE

Form Approved
OMB No 0704-0188

1a REPORT SECURITY CLASSIFICATION Unclassified	1b RESTRICTIVE MARKINGS
2a SECURITY CLASSIFICATION AUTHORITY	3 DISTRIBUTION / AVAILABILITY OF REPORT Approved for public release; Distribution unlimited
2b DECLASSIFICATION / DOWNGRADING SCHEDULE	
4 PERFORMING ORGANIZATION REPORT NUMBER(S) NPS-MA-93-010	5 MONITORING ORGANIZATION REPORT NUMBER(S) NPS-MA-93-010
6a NAME OF PERFORMING ORGANIZATION Naval Postgraduate School 6b OFFICE SYMBOL (If applicable) MA	7a NAME OF MONITORING ORGANIZATION Naval Postgraduate School
6c ADDRESS (City, State, and ZIP Code) Monterey, CA 93943	7b ADDRESS (City, State, and ZIP Code) Monterey, CA 93943
8a NAME OF FUNDING / SPONSORING ORGANIZATION National Research Council 8b OFFICE SYMBOL (If applicable)	9 PROCUREMENT INSTRUMENT IDENTIFICATION NUMBER
8c ADDRESS (City, State, and ZIP Code)	10 SOURCE OF FUNDING NUMBERS PROGRAM ELEMENT NO / PROJECT NO / TASK NO / WORK UNIT ACCESSION NO

11 TITLE (Include Security Classification)
Elastic Curves on the Sphere

12 PERSONAL AUTHOR(S)
Guido Brunnett, Peter E. Crouch

13a TYPE OF REPORT	13b TIME COVERED	14 DATE OF REPORT (Year, Month, Day)	15 PAGE COUNT
Technical	FROM 9-92 TO 11-92	921216	20

16 SUPPLEMENTARY NOTATION

17 COSATI CODES			18 SUBJECT TERMS (Continue on reverse if necessary and identify by block number)
FIELD	GROUP	SUB-GROUP	Elastic curves, geometrically constraint differential equations

19 ABSTRACT (Continue on reverse if necessary and identify by block number)

This paper deals with the derivation of equations suitable for the computation of elastic curves on the sphere. To this end equations for the main invariants of spherical elastic curves are given. A new method for solving geometrically constraint differential equations is used to compute the curves for given initial values. A classification of the fundamental forms of the curves is presented.

20 DISTRIBUTION / AVAILABILITY OF ABSTRACT ☒ UNCLASSIFIED/UNLIMITED ☐ SAME AS RPT ☐ DTIC USERS	21 ABSTRACT SECURITY CLASSIFICATION Unclassified
22a NAME OF RESPONSIBLE INDIVIDUAL Guido Brunnett	22b TELEPHONE (Include Area Code) 22c OFFICE SYMBOL (408)656-2758 MA

Elastic Curves on the Sphere

Guido Brunnett
Department of Mathematics
Naval Postgraduate School

Peter E. Crouch
Center for Systems Science and Engineering
Arizona State University

January 28, 1993

Abstract

This paper deals with the derivation of equations suitable for the computation of elastic curves on the sphere. To this end equations for the main invariants of spherical elastic curves are given. A new method for solving geometrically constraint differential equations is used to compute the curves for given initial values. A classification of the fundamental forms of the curves is presented.

1 Introduction

Two current trends in Geometric Modeling are concerned with

- the development of spline techniques on surfaces (see [14], [12], [10])
- the use of nonlinear spline curves of minimal elastic energy for the modeling of smooth shapes (see [2], [3], [4]).

This paper blends both topics in considering elastic curves on the sphere.

In euclidean space an *elastic curve* can be viewed as an arc length parametrized "cubic" spline in tension, i.e. an elastic curve is a critical point of the functional

$$\Phi(y) = \int_0^l < y'', y'' > + \sigma < y', y' > \, ds \qquad (1)$$

in the space F of smooth maps

$$y : [0, l] \to \mathbf{R}^n, \ |y'| = 1$$
$$y(0) = P_0, \ y(1) = P_1, \ y'(0) = V_0, \ y'(1) = V_1$$

where $P_0, P_1 \in \mathbf{R}^n$, $V_0 \in T_{P_0}\mathbf{R}^n$, $V_1 \in T_{P_1}\mathbf{R}^n$, $\sigma \in \mathbf{R}$ are fixed and l is variable. Expressing y'' in the Frenet frame yields the functional Φ in the form

$$\Phi(y) = \int_0^l (\kappa(s))^2 + \sigma \, ds \tag{2}$$

which explains the interest in elastic curves as those curves that minimize bending.

The notion of cubic splines can be generalized to curves on a Riemannian manifold M by replacing the usual derivative of the tangent vector field y' by the covariant derivative compatible with the metric of M (see [13]). Generalizing the functional (1) in this way, one obtains the concept of elastic curves on arbitrary manifolds. In the case of surfaces embedded in $\mathbf{R}^3$ the algebraic value of the covariant derivative of the tangent vector field y' of a surface curve y is called the geodesic curvature κ_g of y (see [5] and section 2). Therefore we may define an elastic curve on a surface $S : A \subset \mathbf{R}^2 \to \mathbf{R}^3$ as an extremal point of the functional

$$\Phi(y) = \int_0^l (\kappa_g(s))^2 + \sigma \, ds, \tag{3}$$

in the subset $\bar{F}$ of F formed by curves lying on S.

In section 3 a set of differential equations for elastic curves on the sphere is derived. This set includes a differential equation for the geodesic curvature of spherical elastica. Since the normal curvature of a spherical curve is constant, the differential equation for the geodesic curvature suffices to compute the ordinary curvature of a spherical elastica. Furthermore, a formula is given that expresses the squared torsion of a spherical elastica as a rational function of its curvature.

In section 4 we describe the numerical algorithm used to integrate the set of differential equations derived in section 3. The equations have a very particular structure defined by a number of constants of motion, and in particular they constrain the elastic curves to lie on the sphere. We employ an algorithm introduced by Crouch and Grossman [8] which preserves the constraints exactly.

Since Euler's fundamental work on plane elastic curves it is known that these curves can be classified according to their shape. The tools developed in this paper enable us to present the fundamental forms of spherical elastica in the last section.

2 Geometric Preliminaries

Let $S : U \subset \mathbf{R}^2 \to \mathbf{R}^3$ denote a regular parametric surface and N the unit normal vector field of S. A curve $x : I \subset \mathbf{R} \to \mathbf{R}^3$ is a curve on the surface S if and only if $x = S \circ c$ where $c : I \to U$ is a plane curve in U. The unit normal of S along a surface curve x will be denoted by $n := N \circ c$.

The *Darboux frame* b_1, b_2, b_3 along x is the orthogonal frame defined by

$$b_1(t) = \frac{x'(t)}{|x'(t)|}, \quad b_2(t) = n(t) \times b_1(t), \quad b_3(t) = n(t).$$

The equations that express the derivatives b_1', b_2', b_3' in the Darboux basis b_1, b_2, b_3 are given by:

$$b_1' = \omega\kappa_g b_2 + \omega\kappa_n b_3, \tag{4}$$
$$b_2' = -\omega\kappa_g b_1 + \omega\tau_g b_3, \tag{5}$$
$$b_3' = -\omega\kappa_n b_1 - \omega\tau_g b_2 \tag{6}$$

with $\omega(t) = |x'(t)|$.

The *functions* κ_g, κ_n and τ_g are called geodesic curvature, normal curvature and geodesic torsion. The geodesic torsion and the absolute value of geodesic and normal curvature are invariant under reparametrization of the surface.

The geodesic curvature of a surface curve x at a point $x(t)$ is the ordinary curvature of the plane curve generated by orthogonal projection of x onto the tangent plane of S at $x(t)$. It can be computed using the formula

$$\kappa_g = \frac{[x', x'', n]}{|x'|^3}. \tag{7}$$

A surface curve with identically vanishing geodesic curvature is called a *geodesic* of the surface.

The absolute value of the normal curvature of x at a point $x(t)$ is the curvature of the intersection of S with the plane through $x(t)$ spanned by the vectors $x'(t)$ and $n(t)$. While the geodesic curvature is the curvature of a surface curve from a viewpoint in the surface, normal curvature measures the curvature of the curve that is due to the curvature of the underlying surface. If κ denotes the ordinary curvature of the space curve x the identity

$$\kappa^2 = \kappa_n^2 + \kappa_g^2 \tag{8}$$

holds.

The geodesic torsion of a surface curve x at a point $x(t)$ is the torsion of the geodesic that meets x at $x(t)$ with common tangent direction. A *curvature line* of x, i.e. a curve with a tangent vector that points into one of the principal directions of the surface, is characterized by vanishing geodesic torsion.

3 The differential equations of spherical elastica

Let S be a parametrization of a patch on a sphere $\mathbf{S_2} \subset \mathbf{R}^3$ of radius r and center 0 such that

$$S = rN$$

and x be an arc length parametrized (i.e. $|x'| = 1$) curve on S. Then

$$x' = rn' = rb_3'.$$

In this situation (6) implies that

$$\kappa_n = -\frac{1}{r}, \quad \tau_g = 0. \tag{9}$$

Since the absolute value of κ_n and τ_g are invariant under reparametrization, these equations imply that any spherical curve is a curvature line with constant normal curvature.

We consider the variational problem of minimizing

$$\int_0^l (\kappa_g(s))^2 + \sigma \, ds$$

in the space $\bar{F}$ of C^∞ smooth maps

$$y : [0, l] \to \mathbf{S_2}, \ |y'| = 1$$
$$y(0) = P_0, \ y(1) = P_1, \ y'(0) = V_0, \ y'(1) = V_1$$

where $P_0, \ P_1 \ \in \mathbf{S_2}$, $V_0 \in T_{P_0}\mathbf{S_2}$, $V_1 \in T_{P_1}\mathbf{S_2}$, $\sigma \in \mathbf{R}$ are fixed and l is variable.

From (4) one obtains the relation

$$|b_1'|^2 = \kappa_g^2 + \frac{1}{r^2}$$

so that we wish to minimize the functional

$$\int_0^l |b_1'(s)|^2 + \delta \, ds$$

where

$$\delta = \sigma - \frac{1}{r^2}$$

under the constraints

$$|b_1|^2 = 1, \quad b_1 = x', \quad |x|^2 = r^2.$$

Hence, we can apply the Euler-Lagrange equations to the functional

$$F = |b_1'|^2 + \delta + \lambda(|b_1|^2 - 1) + \mu(|x|^2 - r^2) + 2 < \Lambda, x' - b_1 >$$

to obtain the differential equations which govern the extremals:

$$\mu x - \Lambda' = 0 \tag{10}$$

$$\lambda b_1 - b_1'' = \Lambda. \tag{11}$$

Combining these equations yields

$$\lambda' b_1 + \lambda b_1' - b_1''' = \mu x. \tag{12}$$

The derivatives of b_1 expressed in the Darboux basis are given by:

$$b_1' = \kappa_g b_2 - \frac{1}{r} b_3 \tag{13}$$

$$b_1'' = \kappa_g' b_2 - (\kappa_g^2 + \frac{1}{r^2}) b \tag{14}$$

$$b_1''' = (-3\kappa_g \kappa_g') b_1 + (\kappa_g'' - \kappa_g^3 - \frac{1}{r^2}\kappa_g) b_2 + \frac{1}{r}(\kappa_g^2 + \frac{1}{r^2}) b_3. \tag{15}$$

Substituting these derivatives and $x = r b_3$ into (12) and rearranging gives

$$(\lambda' + 3\kappa_g \kappa_g') b_1 + (\lambda \kappa_g - \kappa_g'' + \kappa_g^3 + \frac{1}{r^2}\kappa_g) b_2 - (\frac{\lambda}{r} + \mu r + \frac{1}{r}(\kappa_g^2 + \frac{1}{r^2})) b_3 = 0.$$

Finally, the linear independence of the vectors b_1, b_2 and b_3 implies that

$$\lambda = -\frac{3}{2}\kappa_g^2 + C \tag{16}$$

and

$$\kappa_g'' + \frac{1}{2}\kappa_g^3 - (C + \frac{1}{r^2})\kappa_g = 0. \tag{17}$$

In order to determine the constant C in terms of the tension parameter σ, we consider the boundary condition

$$F(l) - \frac{\partial F}{\partial x'}(l)x'(l) - \frac{\partial F}{\partial b_1'}(l)b_1'(l) = 0$$

for the extremal x. This condition is implied by the fact that the total length l of the curve is variable in the variation (see, e.g., [1]). Thus,

$$-\kappa_g^2(l) - \frac{1}{r^2} + \delta - 2 < \Lambda(l), x'(l) >= 0. \tag{18}$$

Substituting Λ according to (11) into the scalar product $< \Lambda, x' >$ yields

$$\begin{aligned} < \Lambda(l), x'(l) > &= < \lambda b_1(l), b_1(l) > - < b_1''(l), b_1(l) > \\ &= \lambda + (\kappa_g(l))^2 + \frac{1}{r^2} \\ &= -\frac{1}{2}(\kappa_g(l))^2 + \frac{1}{r^2} + C. \end{aligned}$$

Substituting this expression for the scalar product into (18) we obtain

$$C + \frac{1}{r^2} = \frac{1}{2}(\delta - \frac{1}{r^2}). \tag{19}$$

These results are summarized in the following theorem.

Theorem 1 *An elastic curve x under tension σ on the sphere of radius r satifies the differential equations*

$$\begin{pmatrix} x_1' \\ x_2' \\ x_3' \end{pmatrix} = \begin{pmatrix} 0 & 1/r & 0 \\ -1/r & 0 & \kappa_g \\ 0 & -\kappa_g & 0 \end{pmatrix} \begin{pmatrix} x_1 \\ x_2 \\ x_3 \end{pmatrix} \tag{20}$$

where $x_1 = x$, $x_2 = rx'$, $x_3 = x \times x'$ and where the geodesic curvature κ_g of x is a solution of

$$\kappa_g'' + \frac{1}{2}\kappa_g^3 + (\frac{1}{r^2} - \frac{\sigma}{2})\kappa_g = 0. \tag{21}$$

The curvature of a spherical elastic curve can be obtained from (8) and the fact that the normal curvature of spherical curves is constant. The squared torsion of a spherical elastica can be expressed as a rational function of its curvature.

Theorem 2 *The curvature κ and the torsion τ of a spherical elastic curve obey the relation:*

$$r^2\tau^2\kappa^4 = -\frac{1}{4}\kappa^4 - \frac{1}{2}(\frac{1}{r^2} - \sigma)\kappa^2 + \frac{1}{r^2}(\frac{3}{4} - \frac{\sigma}{2}) + C_1.$$

Proof: For the invariants κ and τ of an arc length parametrized curve x in $\mathbf{R}^3$ the relation

$$\tau\kappa^2 = [b_1, b_1', b_1''] \tag{22}$$

holds where [a,b,c] denotes the determinant of three vectors in $\mathbf{R}^3$.

For a spherical curve b_1' and b_1'' can be expressed in the Darboux basis as follows:

$$\begin{aligned} b_1' &= \kappa_g b_2 - \frac{1}{r} b_3 \\ b_1'' &= -(\frac{1}{r^2} + \kappa_g^2) b_1 + \kappa_g' b_2. \end{aligned}$$

Substituting the derivatives into (22) and squaring yields

$$\tau^2\kappa^4 = \frac{1}{r^2}(\kappa_g')^2.$$

Since the differential equation (21) can be integrated to

$$(\kappa_g')^2 = C_1 - \frac{1}{4}\kappa_g^4 - (\frac{1}{r^2} - \frac{\sigma}{2})\kappa_g^2,$$

one obtains the claimed equation using (8).

4 Tracking elastic curves on the sphere

The problem we consider here is that of numerically integrating equations (20) and (21) in Theorem 1. One can of course simply integrate the equations using a standard numerical package, such as an IMSL Runge Kutta routine. However, the system of equations possesses a very special structure. As pointed out in [3], equation (21) may be integrated directly in terms of Jacobi's elliptic functions. We give more details of this process in the next section where we classify the various extremals. As for equation (20) we note that the components of the state vector $[x_1^T, x_2^T, x_3^T]^T$ satisfy algebraic constraints consistent with the fact that the matrix $[x_1, x_2, x_3]$ is simply a multiple r, of a rotation matrix. When a standard integration package is applied to the set of differential equations (20) and (21), these constraints are not preserved exactly, and in particular the norm of the vector x_1 will not remain at the constant value r. This is a particularly important fact when we wish to integrate the equations over a large number of time steps and visualize the resulting curves.

We have therefore made use of a new class of integration algorithms developed by Crouch and Grossman [8], and Crouch, Yan and Grossman [7]

which do indeed preserve such structures. The algorithms are therefore called geometrically exact [6]. We briefly indicate the important aspects of these geometrically stable algorithms which pertain to the equations (20) and (21). Suppose that we wish to numerically integrate an ordinary differential equation on $\mathbf{R}^n$ given by the equations:

$$\dot{x}(t) = F(t, x(t)), \quad x \in \mathbf{R}^n, \quad x(0) = x_0 \tag{23}$$

where

$$F(t, x) = \sum_{j=1}^{N} a^j(t, x) A_j(x) \tag{24}$$

$n \geq N$, A_j are vector fields on $\mathbf{R}^n$ and a^j are functions on $\mathbf{R} \times \mathbf{R}^n$. Suppose that in addition we are given a set of functions on $\mathbf{R}^n$ whose numerical values are constant along solutions of the equation (23) and that the level sets of these functions are manifolds. Denote the level set through x_0 by M. It is convenient to assume the slightly stronger assumption that the vector fields A_j are everywhere tangent to M. We also assume that there is an oracle that can integrate any vector field of the following form, to any desired accuracy:

$$Z(x) = \sum_{j=1}^{N} \alpha^j A_j(x). \tag{25}$$

Here α^j are real numbers. We define vector fields F^p by setting:

$$F^p(x) = \sum_{j=1}^{N} a^j(p) A_j(x)$$

and note that F^p is simply the vector field F with coefficients "frozen" at the point p. If we denote the flow of any vector field Z by $(t, x) \to \theta_Z(t, x)$, $\mathbf{R} \times \mathbf{R}^n \to \mathbf{R}^n$, then since the vector fields A_j are everywhere tangent to M, it follows that $x \in M$ implies that $\theta_{F^p}(t, x) \in M$ for all p and for all t for which the flow is defined.

We now introduce the (explicit) geometrically exact Runge Kutta algorithms as described in [8]. Let $x_k = x(t_k)$ be a point of the integral curve x of (23). Then, define vector fields on $\mathbf{R}^n$ by freezing coefficients of F at various points as follows:

$$F_1(x) = \sum_{j=1}^{N} a^j(t_k, x_k) A_j(x)$$

$$F_2(x) = \sum_{j=1}^{N} a^j(t_k + hc_{21}, \theta_{F_1}(hc_{21}, x_k)) A_j(x)$$

$$F_3(x) = \sum_{j=1}^{N} a^j(t_k + h(c_{31} + c_{32}), \theta_{F_2}(hc_{32}, \theta_{F_1}(hc_{31}, p)))A_j(x),$$

etc. Second, we define the numerical integration algorithm via an update rule:

$$x_{k+1} = \theta_{F_r}(hc_r, \theta_{F_{r-1}}(hc_{r-1}, \cdots, \theta_{F_1}(hc_1, x_k))) \tag{26}$$

where h is the "step length" and c_i and c_{ij} are constants to be determined. These constants are determined from the "consistency equations," obtained by making the Taylor expansions in h, about $h = 0$, of both sides of (26), using on the left hand side the expression $x_{k+1} = \theta_F(h, x_k)$. If the coefficients of h^i agree up to $i = q$, then q is said to be *order* of the resulting algorithm. Note that in general we have $r \geq q$, while for classical Runge Kutta schemes we can always take $r = q$. Note that the update rule defined by equation (26) has the property that if x_k lies in M, then so does x_{k+1} since each flow is defined by a vector field F with frozen coefficients. In the special case where $n = N$, $M = \mathbf{R}^n$ and $A_i = \epsilon_i$ is the standard ith basis vector in R^n, the algorithm reduces to the form of a classical explicit Runge-Kutta algorithm.

In the paper [8] the consistency equations are derived for the geometrically exact Runge Kutta algorithms via a careful geometric analysis of the equations (26). The results show that a geometrically exact third order explicit Runge Kutta algorithm can be obtained for $r = 3$ and is determined by five independent consistency equations, in the six constants defining the algorithm. The equations have multiple solutions, all of which are solutions to the equations which determine the classical explicit Runge Kutta algorithms. Thus, all solutions define classical algorithms, but the solutions are not ones traditionally found in the literature. We have used the following solution of all five equations:

$$c_1 = 1, \quad c_2 = -2/3, \quad c_3 = 2/3,$$

$$c_{21} = -1/24, \quad c_{31} = 161/24, \quad c_{32} = -6.$$

In the special case of the set of equations (20) and (21), defining the elastica on a sphere, we use a hybrid algorithm in which equations (20) are integrated using the third order geometrically exact Runge Kutta algorithm described above by freezing the coefficients κ_g. These coefficients are then updated by integrating equation (21) using elliptic functions.

In equation (20), M is the three dimensional submanifold of $\mathbf{R}^9$ determined by the equations

$$< x_1, x_1 >= r^2, \quad < x_1, x_2 >= 0, \quad < x_1, x_3 >= 0,$$

$$< x_2, x_2 >= 1, \quad < x_2, x_3 >= 0, \quad < x_3, x_3 >= 1.$$

The solutions of (20) for any initial condition $x(0) = x_0 \in M$ lie completely in M. This follows from the fact that the functions

$$f_1 =< x_1, x_1 >, \quad f_2 =< x_1, x_2 >, \quad f_3 =< x_1, x_3 >.$$

$$f_4 =< x_2, x_2 >, \quad f_5 =< x_2, x_3 >, \quad f_6 =< x_3, x_3 >$$

satisfy the system of differential equations

$$\begin{aligned} f_1' &= 2f_2 \\ f_2' &= f_4 + \kappa_g f_3 - (1/r^2) f_1 \\ f_3' &= f_5 - \kappa_g f_2 \\ f_4' &= 2\kappa_g f_5 - (2/r^2) f_2 \\ f_5' &= \kappa_g f_6 - (1/r^2) f_3 - \kappa_g f_4 \\ f_6' &= -2\kappa_g f_5 \end{aligned}$$

which has the unique solution

$$f_1 = r^2, \ f_2 = 0, \ f_3 = 0, \ f_4 = 1, \ f_5 = 0, \ f_6 = 1.$$

Since this argument does not specify the function κ_g, it follows that the flows of the vector fields $F_1 - F_3$ with frozen coefficients are mappings into M as needed in formula (26).

Furthermore, the vector fields A_j in equation (20) are linear, so that F is given by an expression of the form

$$F(x) = \sum_{j=1}^{N} b^j(t, x) B_j x \tag{27}$$

where B_j are matrices and b^j are functions. Freezing the functions b^j to values β^j yields a system of linear differential equations with constant coefficients:

$$\dot{x} = \Big(\sum_{j=1}^{N} \beta^j B_j \Big) x. \tag{28}$$

Thus, the flow θ_{F_i} of the vector field F_i (i=1,2,3) is given by

$$\theta_{F_i}(t, q) = \exp(tC_i)\, q$$

and (26) takes the special form

$$x_{k+1} = \exp(c_3 h C_3) \cdot \exp(c_2 h C_2) \cdot \exp(c_1 h C_1) \cdot x_k.$$

Since $b^1 = 1/r$ is constant and $b^2 = \kappa_g$ depends only on t, the matrices C_i are given by

$$C_1 = C(t_k), \quad C_2 = C(t_k + hc_{21}), \quad C_3 = C(t_k + h(c_{31} + c_{32}))$$

where $C(t) := \sum_{j=1}^{2} b^j(t) B_j$. C can be considered as a 3×3 skew symmetric matrix with matrix components that are themselves 3×3 matrices. Therefore the standard formula for the exponential of a 3×3 skew symmetric matrix can be used to compute the flow of each vector field:

$$\exp(t\phi S(c)) = I + \sin(t\phi) S(c) + (1 - \cos(t\phi)) S(c)^2$$

where $S(c)$ is the skew symmetric matrix satisfying $S(a)b = b \times a$, and $|c| = 1$.

Regarding the performance of the geometrically stable integration method it is clear that this method is computationally more expensive than a classical algorithm with the same number of stages and step length. The exact cost of the new integration scheme can be found in [6]. However, if we compare the performance of the geometrically stable method with the classical fourth order Runge-Kutta algorithm on the problem of spherical elastica, it turns out that a slightly increased step length for the new method suffices to outperform the classical integration method. Using MATLAB implementations of both algorithms we found that the geometrically stable method needs an average value of 1001 Mflops for one complete step while the fourth order Runge-Kutta only uses an average value of 768 Mflops per step. Therefore, one can statistically achieve the same performance by using an increased step length of $h \approx 1.3038\, h_{RK}$ for the new method. Taking into account that the proposed algorithm not only delivers points that lie exactely on the sphere but that are also approximately equally spaced along the tracked curve, the geometrically stable method seems to be a good choice for the integration of spherical elastica.

A performance comparison of the new integration scheme with a more sophisticated classical method, the IMSL Runge Kutta implementation, can be found in [7].

5 Classification of spherical elastica

Acting on the suggestion of D. Bernoulli, L. Euler derived differential equations for plane elastica and classified the fundamental forms of these curves (see [9], [11]). A curvature analysis of the various fundamental cases has been given in [3].

In this section we classify the forms of spherical elastica based on the differential equation (21) for the geodesic curvature. This equation is of the

same form as the equation for the curvature of plane elastica and can be solved in terms of Jacobi's elliptic functions in the form:

$$\kappa_g(s) = \kappa_m \, \mathrm{dn}(\kappa_m(s - s_m)/2 \,|\, l^2)$$

where the positive parameter l^2 of the elliptic function is given by

$$l^2 = \frac{2(\kappa_m^2 + 2/r^2 - \sigma)}{\kappa_m^2} \tag{29}$$

(see [3]). The parameter κ_m represents the amplitude of the periodic curvature function and s_m denotes the value at which $\kappa(s_m) = \kappa_m$.

To obtain a representation of the curvature in terms of Jacobi's functions with parameter l^2 smaller than 1, one uses the formula

$$\kappa_g(s) = \kappa_m \, \mathrm{cn}(\sqrt{(\kappa_m^2 + 2/r^2 - \sigma)/2}(s - s_m) \,|\, \frac{1}{l^2}) \tag{30}$$

if $\sigma < 0.5\kappa_m^2 + 2/r^2$. Since the function cn has zeros while dn is positive, the above case distinction reflects the main division of elastic curves into those where the geodesic curvature changes sign and the other with constant sign of their geodesic curvature.

The change of the forms of spherical elastica while κ_m is fixed and σ increases is shown by figures 1-8. The maximum value of the tension parameter σ for a real elastic curve on a sphere is according to (29) $\sigma = \kappa_m^2 + 2/r^2$. This choice of σ corresponds to the dashed circle that is shown in all figures for the purpose of orientation. The second curve in figure 1 has a negative tension parameter of high absolute value ($\sigma = -10000$). In comparison to figure 2 where $\sigma = -30$ we observe that decreasing the tension parameter has the effect of lowering the amplitude of the curve as it is known from the euclidean case (see [3]). The oscillation of the curve in figure 1 is of too low amplitude to be visually observed and the curve can not be distinguished from the geodesic determined by the initial conditions. (Note, that the geodesic curvature (30) is far from getting flat for $\sigma \to -\infty$ but in fact approaches a cos function that oscillates with a period that decreases with σ.)

A curve with positive tension parameter is shown in figure 3 where $\sigma = 2/r^2 = 2$. The displayed curve is a special case because the parameter $1/l^2 = 1/2$. Here the geodesic curvature is given by the lemniscate function:

$$\kappa_g(s) = \kappa_m \, \mathrm{coslemn}(\kappa_m(s - s_m)/2).$$

In figures 4 and 5 it is illustrated that with increasing positive σ the bays of the curves start to overlap until a figure-8-configuration is reached

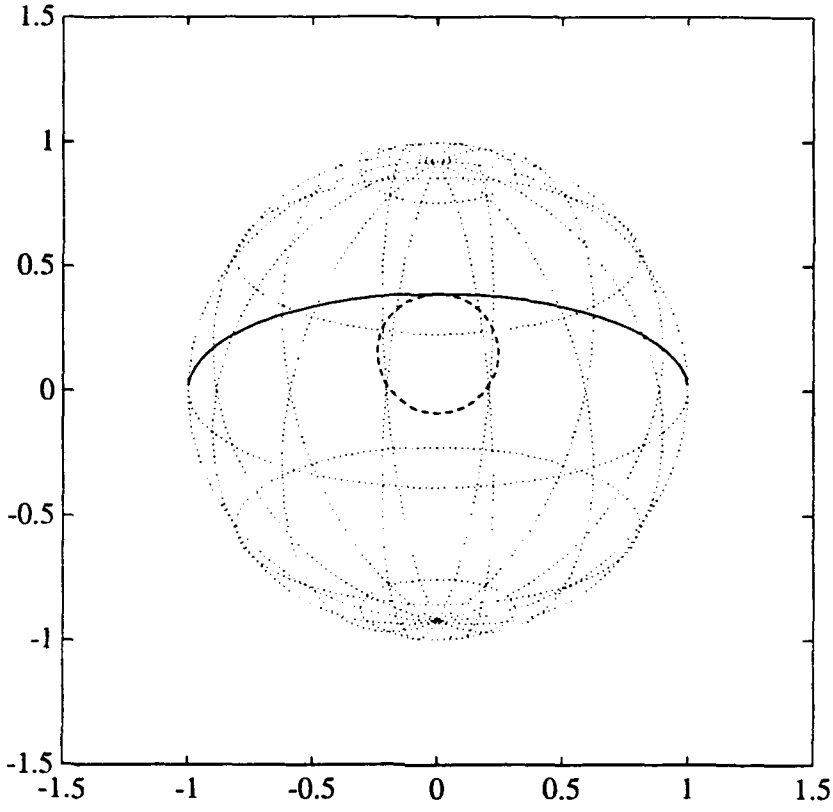

Figure 1: $\kappa_m = 4$, $\sigma = -10000$

where all double points of the curve coincide. This happens for a parameter $\sigma \approx 7.849$.

While σ increases further the curve proceeds through the figure-8-shape forming a series of loops with alternating sign of geodesic curvature (see figure 6). These loops recede from each other until in the limiting case, when $\sigma = 2/r^2 + 0.5\kappa_m^2$, the curve forms a single loop (see figure 7). Here the geodesic curvature is given by

$$\kappa_g(s) = \kappa_m \mathrm{sech}(\kappa_m(s - s_m)/2).$$

Figure 8 shows that the single loop transforms into a series of loops with the same sign of geodesic curvature. With increasing σ the loops come closer together and finally collapse into a circle when $\sigma = 2/r^2 + \kappa_m^2$.

References

[1] O. Bolza. *Vorlesungen über Variationsrechnung.* Koehler und Amelang, Leipzig, 1949.

[2] G. Brunnett. *Properties of Minimal Energy Splines.* Curve and Surface Design, H. Hagen (ed.), pp. 3-22., SIAM 1992.

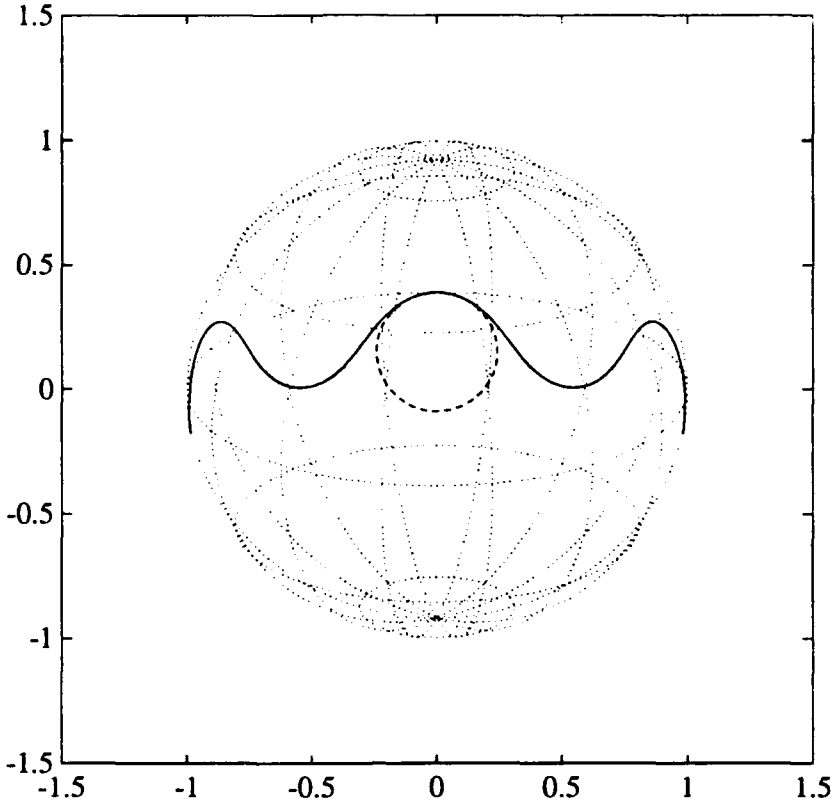

Figure 2: $\kappa_m = 4$, $\sigma = -30$

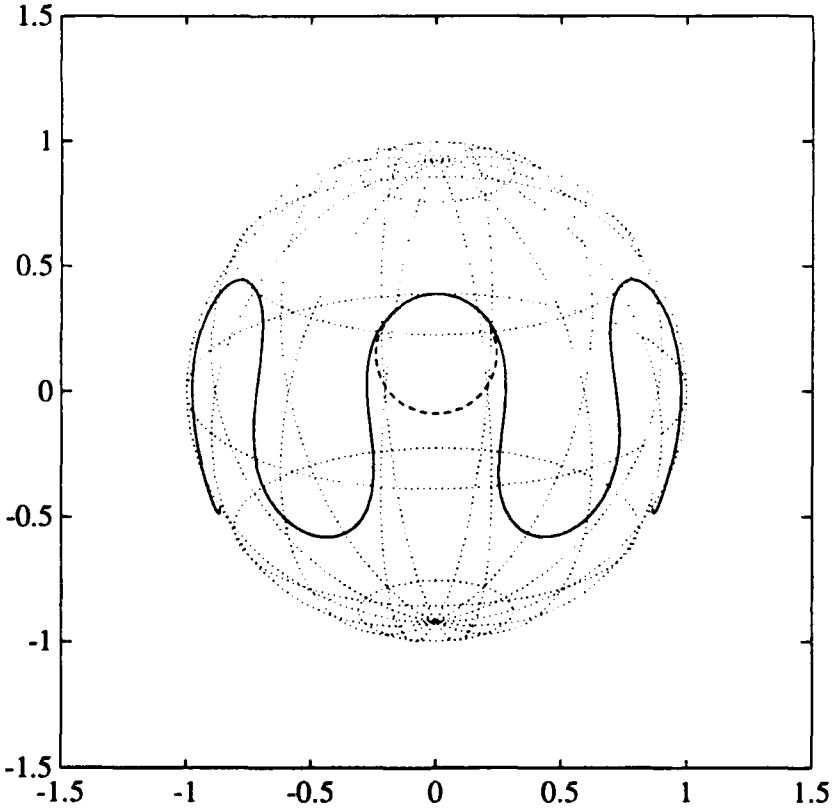

Figure 3: $\kappa_m = 4$, $\sigma = 2$

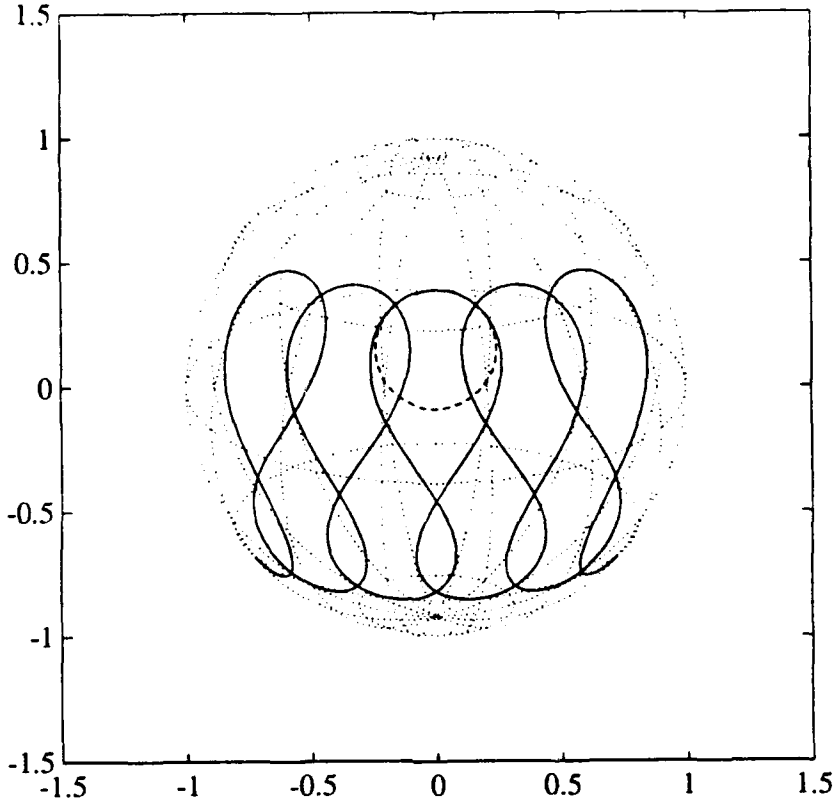

Figure 4: $\kappa_m = 4$, $\sigma = 6.8$

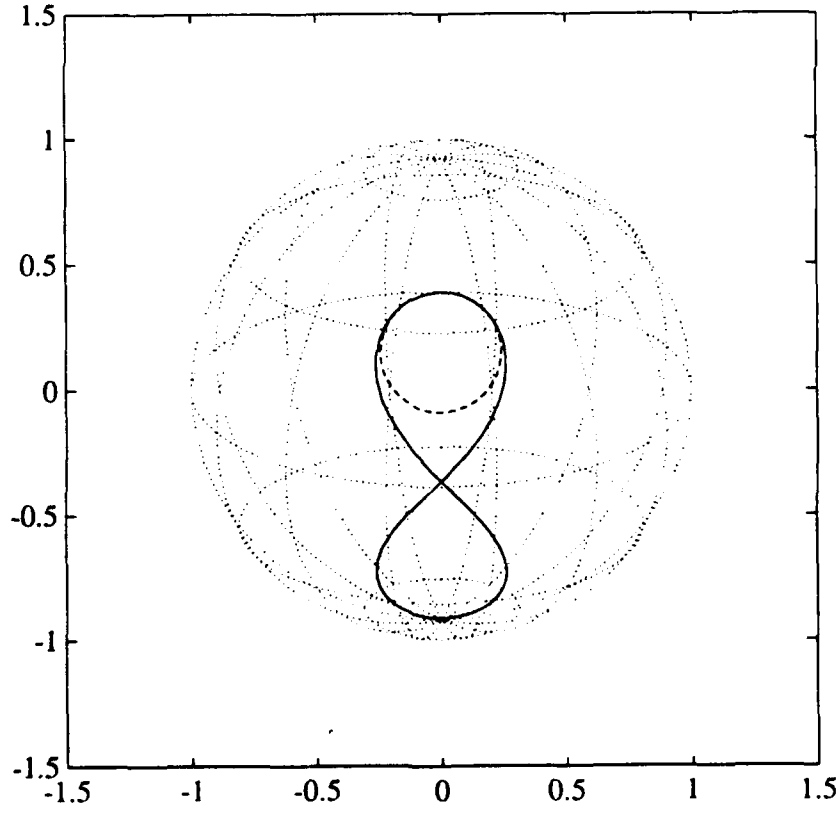

Figure 5: $\kappa_m = 4$, $\sigma = 7.8489$

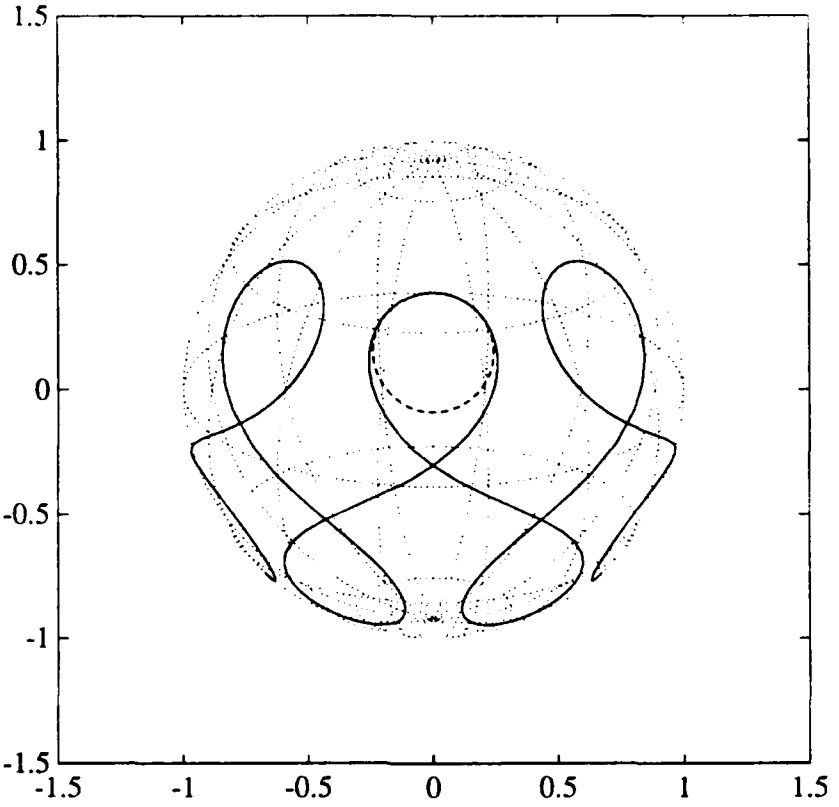

Figure 6: $\kappa_m = 4$, $\sigma = 9.04$

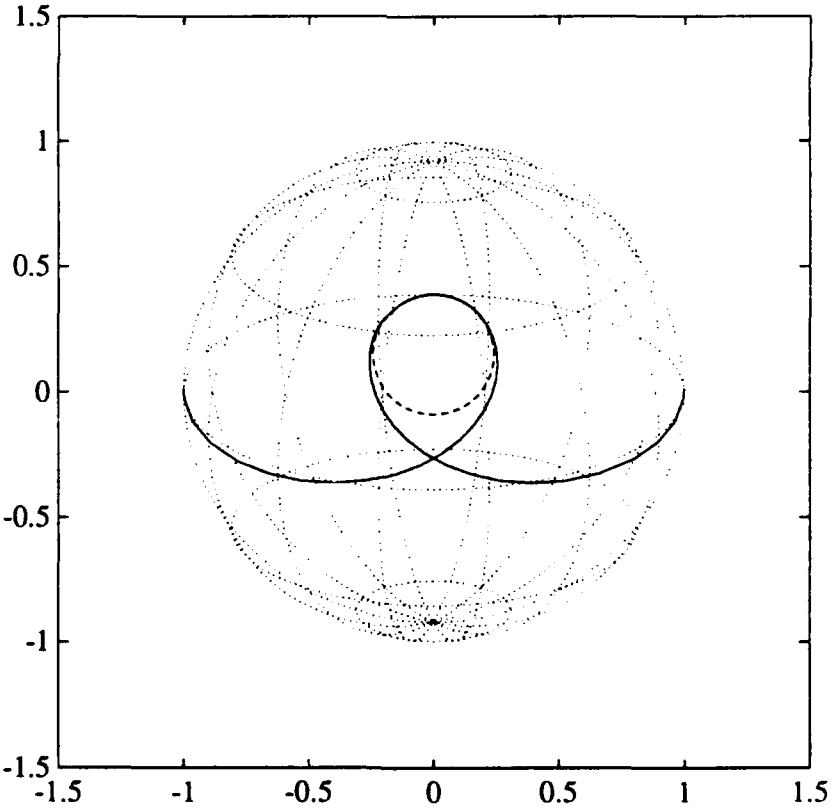

Figure 7: $\kappa_m = 4$, $\sigma = 10$

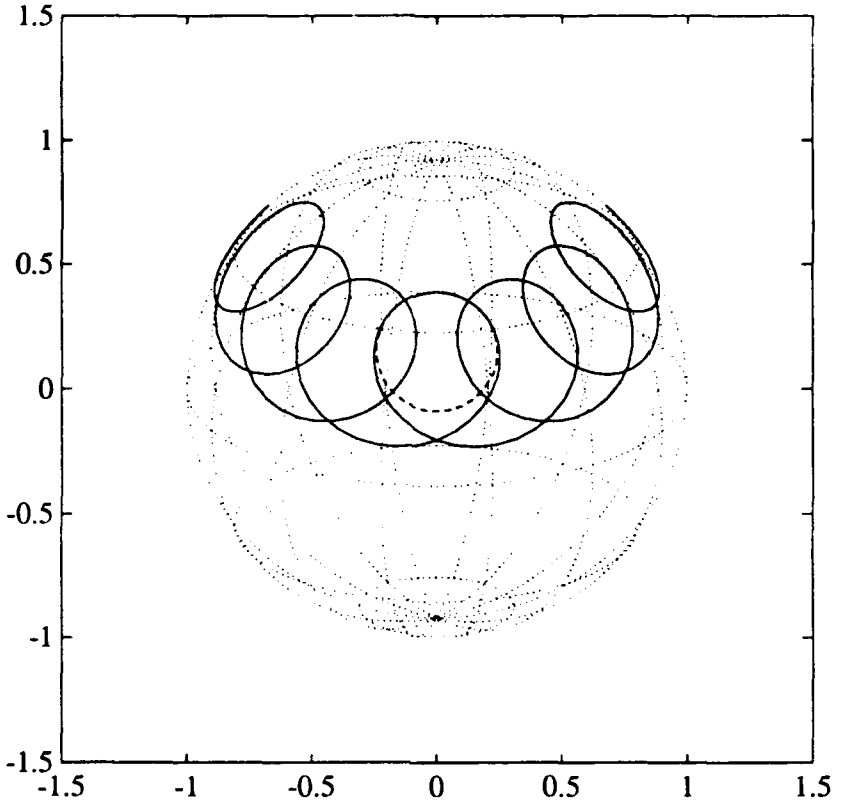

Figure 8: $\kappa_m = 4$, $\sigma = 11.92$

[3] G. Brunnett. *A New Characterization of Plane Elastica.* Mathematical Methods in Computer Aided Design II, T. Lyche and L. Schumaker (eds.), pp.43-56, Academic Press 1992.

[4] G. Brunnett and J. Kiefer. *Interpolation with Minimal Energy Splines.* Submitted to CAD.

[5] M. P. do Carmo. *Differential Geometry of Curves and Surfaces.* Prentice Hall, 1976.

[6] P.E. Crouch, R. Grossman, and Y. Yan. *A Third Order Runge Kutta Algorithm on a Manifold.* Submitted to BIT, 1992.

[7] P.E. Crouch, Y. Yan and R. Grossman. *On the Numerical Integration of the Dynamic Attitude Equations.* to appear in the proceedings of the IEEE CDC Conferene, Tucson, Arizona, 1992.

[8] P.E. Crouch and R. Grossman. *Numerical Integration of Ordinary Differential Equations on Manifolds.* To appear in J. of Nonlinear Science, 1991.

[9] L. Euler. *Additamentum De curvis elasticis.* Methodus Inveniendi Lineas Curvas Maximi Minimive Proprietate Gaudentes, Ser. 1., Vol. 24, Lausanne 1744.

[10] J. Hoschek and G. Seemann. *Spherical Splines.* Mathematical Modeling and Num. Anal., 26 (1), pp. 1-22, 1992.

[11] A.E.H. Love. *A Treatise on the Mathematical Theory of Elasticity.* 4th. ed., Cambridge University Press, 1927.

[12] G. Nielson. *Bernstein/Bezier Curves and Splines on Spheres based upon a Spherical De Casteljau Algorithm.* Technical Report TR-88-028. Arizona State University.

[13] L. Noakes, G. Heinzinger and B. Paden. *Cubic Splines on Curves Spaces.* IMA J. Math. Control & Inform. 6, pp. 465-473, 1989.

[14] K. Shoemake. *Animating Rotation with Quaternion Curves.* ACM Computer Graphics, 19 (3). Proc. Siggraph'85, pp. 245-254. 1985.

[15] K. Strubecker. *Differentialgeometrie I-III.* Sammlung Göschen, de Gruyter, Berlin 1969.

DISTRIBUTION LIST

Director (2)
Defense Tech Information Center
Cameron Station
Alexandria, VA 22314

Research Office (1)
Code 81
Naval Postgraduate School
Monterey, CA 93943

Library (2)
Code 52
Naval Postgraduate School
Monterey, CA 93943

Professor Richard Franke (1)
Department of Mathematics
Naval Postgraduate School
Monterey, CA 93943

Dr. Neil L. Gerr (1)
Mathematical Sciences Division
Office of Naval Research
800 North Quincy Street
Arlington, VA 22217-5000

Dr. Richard Lau (1)
Mathematical Sciences Division
Office of Naval Research
800 North Quincy Street
Arlington, VA 22217-5000

Carl de Boor (1)
Department of Computer Science
University of Madison-Wisconsin
Madison, WI 53706

Guido Brunnett (15)
Department of Mathematics
Naval Postgraduate School
Monterey, CA 93943